Physica D 66 (1993) 299–307

PHYSICA D

some cases using interval arithmetic) of the con-

Though many have attempted to generalize

more than two degrees of freedom, or equivalently, symplectic maps of four or more dimensions, there has been limited success in determin-

approximations to invariant tori have been obtained [14,25], and computations reveal that the

studies is number theoretic; there is no satisfac-

theory to simultaneous approximation of several

because their continued fraction expansions are eventually periodic (these give rise to self-similar structures). Finally, the most robust tori appear to correspond to the class of quadratic irrationals known as the noble numbers; these have a con-

Roughly speaking, the explanation for this is that

There has been some speculation that for four-

therefore cubic [11,12]. However, even in this

self-similar behavior near breakup [21], and there is no evidence that cubic irrationals are more robust than others.

complex, symplectic map corresponding to the coupling of two semi-standard maps was intro-

Fourier series for the semi-Froeschlé map, we are

holomorphic functions of several complex vari-

2. Coupling of two semi-standard maps

The semi-standard area-preserving map was

numerically simpler model than the standard the semi-standard map takes $\{x_{t-1}, x_t\} \mapsto$

$$\delta^2 x_t \equiv x_{t+1} - 2x_t + x_{t-1} = \mathrm{i}a\, \mathrm{e}^{\mathrm{i}x_t}\,; \qquad (1)$$

this is a map. The notation δ^2 is reminiscent of the second derivative operator.

In this paper we study a four-dimensional

$$F(x) \equiv \mathrm{i}(\ldots a_2\, \mathrm{e}^{\ldots}) \qquad (3)$$

There are three parameters, the strength of the (a_1, a_2) and ϵ, the strength of the coupling of the two maps. Eq. (2) is symplectic since F is the gradient of a scalar potential (see for example [14]).

We are looking for solutions x_t of eq. (2) that

torus be analytically conjugate to a uniform rota-

$$x_t \longrightarrow x_{t+1}$$

Thus, for a given ω, an invariant torus for eq. (2) is given by

$$x_t = x(\theta + 2\pi\omega t)\,, \qquad (5)$$

thus $x(\theta)$ is coperiodic with θ:

$$x(\theta) = \theta + \chi(\theta)\,,$$

where $\chi(\theta)$ is doubly 2π-periodic. If we suppose

eq. (5) into eq. (2) yields the Percival form of the mapping

$$\delta^2 x(\theta) = x(\theta + 2\pi\omega) - 2x(\theta) + x(\theta - 2\pi\omega) = F(x(\theta))\,. \qquad (8)$$

equations determining the Fourier coefficients χ_n; these will be obtained in section 4.

3. Incommensurate frequencies

in [10,27,25]. In particular, rather sophisticated

for which there is an analytic invariant circle with frequency ω. Here a^{ss}, the critical function, is zero for every rational value and exhibits a maximum for

The critical function appears to have a local maximum at each of the *noble frequencies*: those equivalent to γ under a modular transformation, or equivalently which have a continued fraction

These results also apply to the semi-Froeshlé map when $\epsilon = 0$. Thus an invariant torus of

KAM theory implies that for sufficiently small

quency vector satisfies a Diophantine condition.

tors $\mathcal{D}_\mu$ consists of those $\omega \in \mathbb{R}^d$ for which there exists a $C > 0$ such that for all $(p, q) \in \mathbb{Z}^{d+1}$

$$|p \cdot \omega - q| \geq \frac{C}{\|p\|^{\mu}} , \tag{11}$$

K

If $d = 1$ then K can be replaced by $1/\sqrt{5}$ but nothing smaller.

Diophantine are those constructed from alge-

Recall that an algebraic field generated by $\xi \in \mathbb{R}$ of degree n is defined as the set of numbers of the form

$$R(\xi) = \frac{P(\xi)}{\cdots}$$

$$\sigma \in \sqrt{2} = [2, 2, 2, 2. \ldots] \equiv [2^\infty] ,$$

$$\zeta \equiv \frac{1+\sqrt{2}}{5+4\sqrt{2}} = [0, 4, 2^\infty] . \qquad (13)$$

The expressions on the right hand sides above give the continued fraction expansions. Setting [illegible]

[illegible]

easy to see, since $\xi^4 - 14\xi^2 + 9 = 0$ and any polynomial in ξ has the form $P(\xi) = a + b\sqrt{2} +$ $c\sqrt{5} + d\sqrt{10}$ for a, b, c, $d \in \mathbb{Z}$. Thus γ, σ, and ζ [illegible]

Finally we consider a cubic irrational, the real

$\tau \simeq$ [illegible] 809 734 [illegible]

$$[1, \ldots$$ [illegible]

$$5, 1, 2, 8, 2, 1, 1, 3, 1, \ldots] . \qquad (14)$$

This so called "spiral mean" frequency was in- [illegible]

elements appear unbounded [22]. None-the-less, [illegible]

τ is the smallest of the "PV numbers", which [illegible]

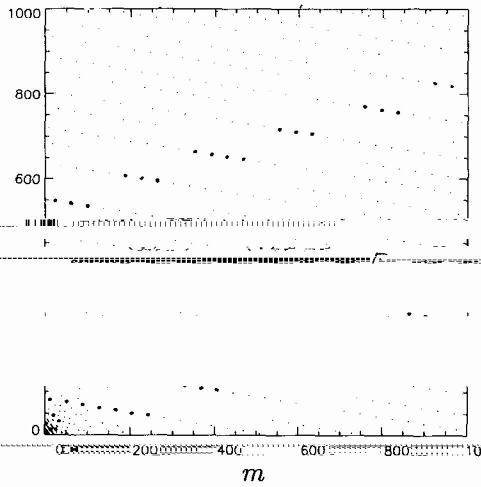

Fig. 1. [illegible] peaks in the inverse of the smallest denominator [illegible] $\omega = (\gamma, \sigma)$. Values of $(\mathcal{D}_{(m,n)}(\gamma; \sigma) \| (m, n) \|)^{-1} \geq 1.0 \times 10^{\ldots}$ [illegible]

$$\ldots \mathcal{D} \ldots = 4 \sin^2(\ldots) \ldots 1.32\,471\,795\,724\,474\,602\,596\,090\,885\,44\ldots \qquad (15)$$

[illegible]

pect the Fourier coefficients to have similar isolated peaks [illegible]

[illegible] fortunately not the case.

$u = (\ldots) = (\ldots)$. (16)

our expansions. Further, using eq. (7) we define

$$g(u) = \mathrm{i}[x(\theta) - \theta] = \mathrm{i}\chi(\theta) . \qquad (17)$$

be needed in the Fourier expansion of $\chi(\theta)$, $g(u)$ has a Taylor expansion

$$g(u) = \sum b_n u^n$$

Here we use standard multi-index notation for the vector exponentiation: while $u \in \mathbb{C}^2$ and $n \in \mathbb{N}^2$, $u^n = u_1^{n_1} u_2^{n_2} \in \mathbb{C}$. In addition to the expansion of g, we will need the expansions of its exponen-

$$\mathrm{e}^{g_i(u)} = \sum c_n^{(i)} u^n , \qquad (19)$$

$$-k \left(u_1 u_2 \, \mathrm{e}^{\ldots} \right) . \qquad (20)$$

If ω is incommensurate, then D_n is nonzero, so

define the partial order $\leq$ on integer vectors by

A simple derivative identity allows us to find the coefficients

$$\frac{\mathrm{d}}{\mathrm{d}u_j} \mathrm{e}^{g_i(u)} = \left(\frac{\mathrm{d}}{\mathrm{d}u_j} g_i(u) \right) \mathrm{e}^{g_i(u)} \qquad (23)$$

$$n_j c_n^{(i)} = \sum_{m \neq (0,0)}^{n} m_j b_m^{(i)} c_{n-m}^{(i)} \qquad (24)$$

Note that eq. (24) allows the two forms, $j = 1$ or 2, for n off the axis (these are equivalent), but for n on the axis, only one is valid because of a examination of the mapping eq. (25) yields in addition

$b^{(2)} = 0$, $b^{(1)} = 0$ (26)

$b^{(2)}$ and $b^{(2)}$ are identical to those for the

respectively.

g, the domain of convergence of $g(u)$ is the

each component's series.

$$S = \sum b_m z^m , \tag{28}$$

similar to the series obtained in the previous

projection onto the radius space is denoted Π:

Several types of subsets of $\mathbb{C}^d$ are of interest.

interior of the set of points for which it converges absolutely. A *polydisk* is the appropriate

$d\}$. A *Reinhardt domain* is a domain R

such that

main is *complete* if for every $z \in R$ the polydisk

points with smaller radii. Finally a domain D is

is a convex subset of $\mathbb{R}^d$.

terms at a point z then it converges absolutely to a holomorphic function. The domain of convergence, D, of S is the interior of the set for which $|b_m z^m|$ is bounded. Furthermore D is a log

ly, if $|b_m z^m|$ is unbounded then there is an order-

Its most unusual aspect is that the domain of

in more detail. Suppose $z, x \in \mathbb{C}^{d*} \cap D$. Then for $\alpha + \beta = 1$ let u be any point in $\mathbb{C}^{d*}$ such that

where r_i and s_i are the radii of z and x, respectively.

x. $B = \sup(|b_m z^m|, |b_m x^m|)$ exists, and straightforward since the series eq. (18) has the desired form; it yields the intersection result

Corollary 1. For fixed k defined by eq. (21), an analytic invariant torus with Diophantine fre-

function $r_1(r_2)$ or $r_2(r_1)$.

tion of these domains is possible with reasonable

6. Numerical results

the ith component is

$$\log(r_1^{(i)}(s)) = -\lim_{n\to\infty} \frac{\log \ldots_n (s)}{n} \tag{36}$$

for each fixed s. Since the domain of conver-

factor of ten in computing time over using the

lead us to choose $N = 255$ as our matrix di-

of the Fourier coefficients. We first consider $\omega = (\gamma, \sigma)$ where the components were defined by eqs. (10) and (13). Fig. 2 is a logarithmic

jump. This can be seen in the contour plot as a

coefficients for greater m are influenced by this

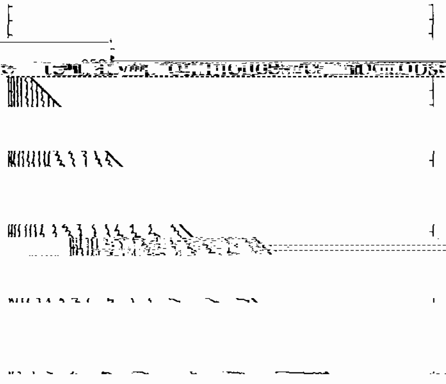

Fig. 2. Logarithmic contour plot of the Fourier coefficients $b^{(1)}_{...}$, where $\omega = (\gamma, \sigma)$ and $k = 0.2$. Here $0 \le b^{(1)}_{...} \le 10^{150}$.

evaluate for this problem as it could be in gener-

$(\log[B_n(s)], n)$ are due to near commen-

By contrast, the Fourier coefficients for the

denominator and the single previous coefficient

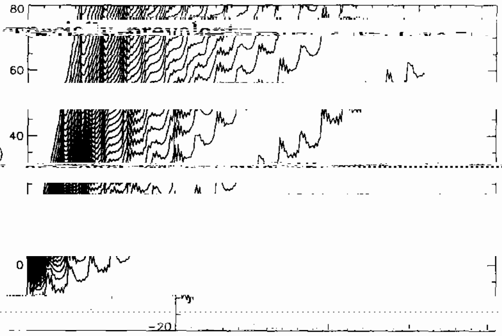

tremely important, and primary, secondary, and

that the Fourier coefficients have an extremely

to float by $n = 10$ points each, and the fit with the lowest residual was automatically chosen. This eliminates the problem of a given fit falling just

which leads us to expect at least 2 decimal

Using the three frequency pairs, $\omega = (\gamma, \sigma)$,

These domains of convergence are displayed in

$B^{(2)}$ as dashed curves.

(γ, σ) on a log–log scale. This example shows

The sharp bends seen in some of the curves are due to the regular spacing of angles on a grid,

near the axes.

for the first component, $B_n^{(1)}$ (solid curves).

standard map with frequency ω_1. We call the r_1 axis the "dominant" axis for $B_n^{(1)}$; similarly,

various curves intersect the dominant axis at

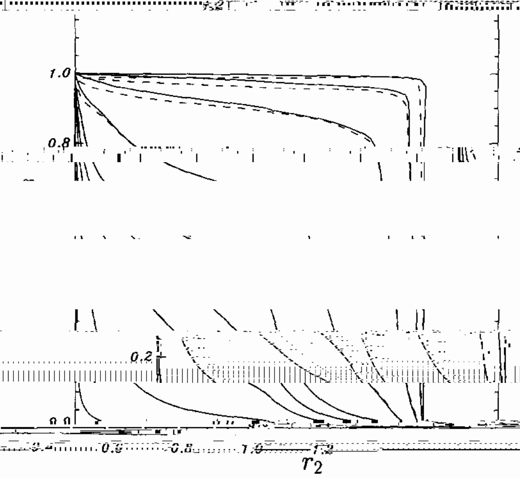

Fig. 4. Boundary of the domain of convergence for $\boldsymbol{\omega} =$ [illegible]

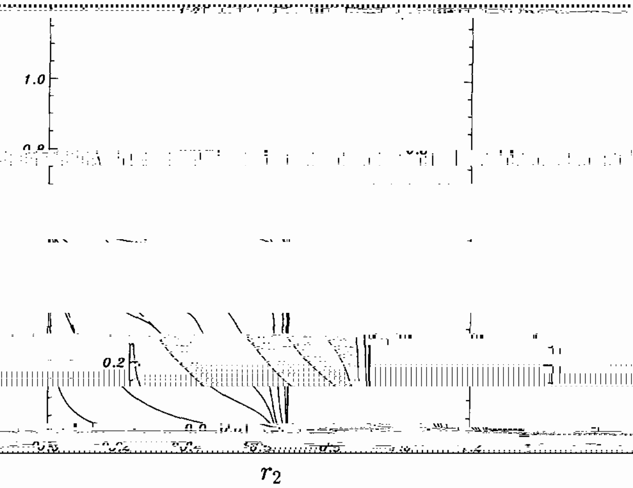

Fig. 6. Same as fig. 4 with $\boldsymbol{\omega} = (\tau, \tau^2)$.

corresponds to the frequency $\omega_1 = \gamma$, and the horizontal to [illegible]

frequencies. Note that the curves in figs. 4 and 6 [illegible]

[illegible] for example in fig. 4, the intersection with the r_2 axis occurs near 0.985, while table 1 implies that the correct value is 0.966. This overestimate is due to the fact that we compute the coefficients only out to the 255th Fourier

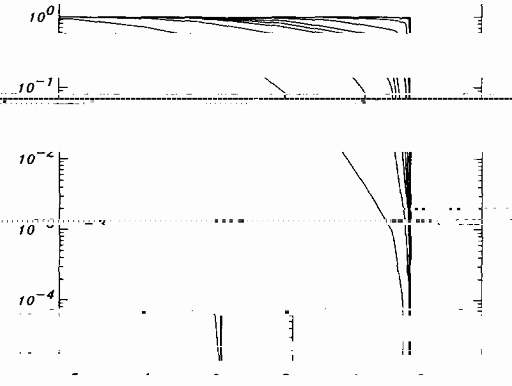

Fig. 7. Same as fig. 4 except on a log–log scale.

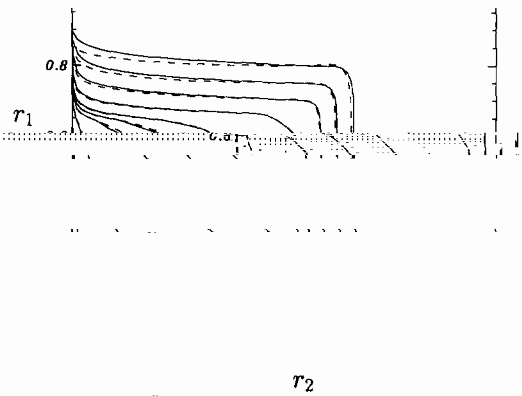

Fig. 5. Same as fig. 4 with $\boldsymbol{\omega} = (\gamma, \zeta)$.

Table 1

Critical values for the semi-standard map.

$\gamma + \zeta$	0.00

ate evaluation of the critical function. For our

r_1 axis appears to be much lower than the value

actually rise rapidly to the correct (actually over-estimated) value as $r_2 \to 0$. It is interesting that in this case even through the values on axis are

$r_1^{(1)} = a^{ss}(\omega_1)$, independent of r_2; the numerical

limits to $a^{ss}(\omega_2)$ on the r_2 axis. This also occurs for the domain of convergence of the second component $B^{(2)}$:

$$B_n^{(2)}(s) \simeq sk \frac{D_{(n,0)}}{D_{\dots}} b_{(n,0)}^{(1)} . \quad (38)$$

bounded by the rectangle

scheme for finding $r_1(r_2)$ when k is small, we

Fig. 8 displays the coefficients $B_n^{(1)}$ and $B_n^{(2)}$ for $s = 10^{-25}$ and $\omega = (\gamma, \sigma)$. In the limit of small

spikes and valleys corresponding to a compli-

profile approaches a limiting form as $s \to 0$, even though the magnitude of $B^{(2)}$ approaches zero. Likewise, $B_n^{(2)}$ near the r_2 axis yields the semi-

to zero, while similarly converging to a fixed

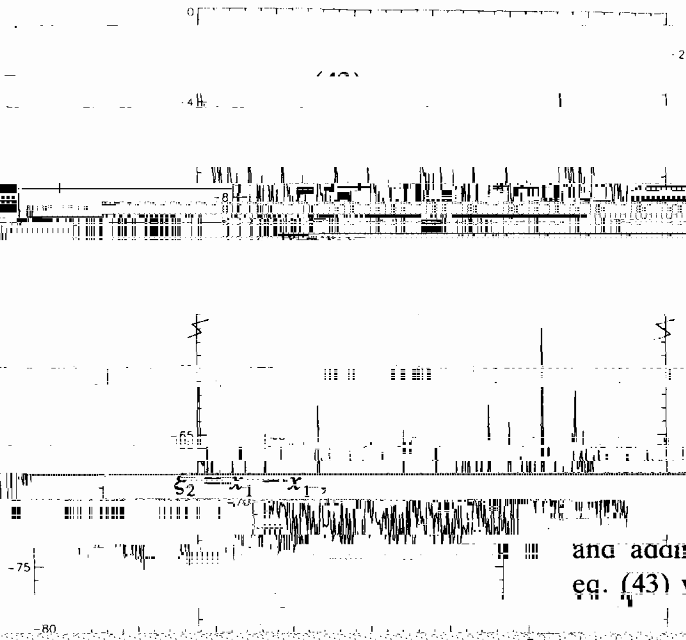

accord with eq. (38).

main for any finite k. This follows from the

the fact that the curves limit to the semi-standard values on the axes. This fact can be used as an upper-bound when discussing the question of which torus is "last".

We also computed $r_1(r_2)$ curves for negative

$a^{ss}(\omega_2)$. Otherwise the curves are qualitatively similar to those shown in figs. 4–6, so we omit

mined by the positive k results.

large k limit corresponds to

Defining the new variables

$$\xi_1 = x_1 + x_2 , \tag{44}$$

$$\xi_2 = x_1 - x_1 , \tag{45}$$

and adding and subtracting the components of eq. (43) yields a new map:

(ξ_1, ξ_2) up to some critical value

Now eq. (43) is approximately valid for small a_1

$$r_1 r_2 = \frac{a^{ss}(\omega_1 + \omega_2)}{2k} , \tag{48}$$

which defines a hyperbola.

$$a_1 \le a^{ss}(\omega_1) , \quad a_2 \le a^{ss}(\omega_2)$$

rived. As a confirmation, table 1 shows that more quickly than for other ω curves, as we ...

for finding $r_1(s)$ has numerical problems when $k \ll 1$. For such small k, the singularity on one axis is dominant over the singularity on the other axis. To illustrate the problem, consider a simple example which as a similar imbalance in the prominence of its singularities. Let

$$\ldots \quad \alpha - r_1 \quad \beta - r_2 \quad \sum_{m,n} \ldots \qquad (50)$$

Here small values of δ simulate small values of k; ... convergence of this series is the rectangle ...

We examine the behavior of eqs. (34)–(36) when applied to eq. (50) by a perturbation analysis near $s = 0$. For a finite n, the algorithm gives an error in r_1 of

$$\Delta r_1 \sim -\frac{\delta\alpha}{n}\left(\frac{\alpha s}{\beta}\right)^n \qquad (51)$$

Thus the method works well provided $s < \beta/\alpha$ ...

... tions, the slope is never larger than one, we switch to the inverse of the slope when $s = 1$. Thus, supposing $\beta < \alpha$ the method fails in a cone ...

below 10^{-5} in the computations.

... terms of the coupling parameter ϵ, instead of k. ... three dimensional graphs seen in figs. 9 and 10. ... sum frequency $\omega_1 + \omega_2$ through eq. (49). Numerical overflow for large k prevents us from calculating the curves for ϵ too close to its maximum value.

In many ways, it is these three-dimensional ...

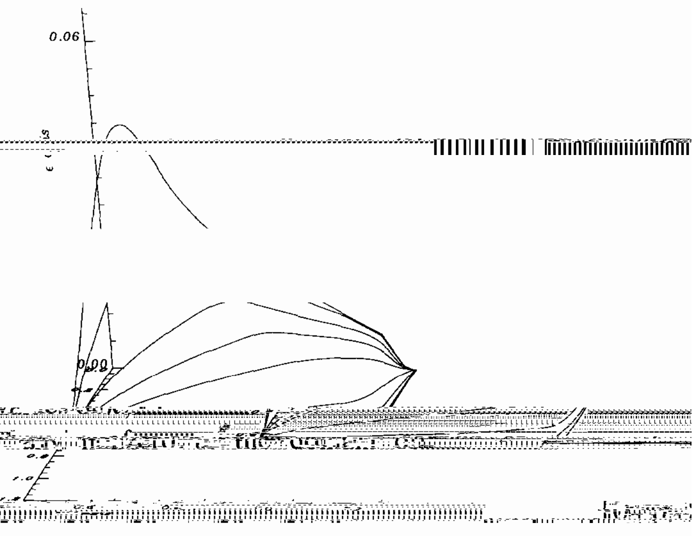

Fig. 9. Radii of convergence curves in (ϵ, s, r) space for ... and $\omega = (\tau, \tau^2)$ where r_1 corresponds to the frequency τ, and r_2 to τ^2.

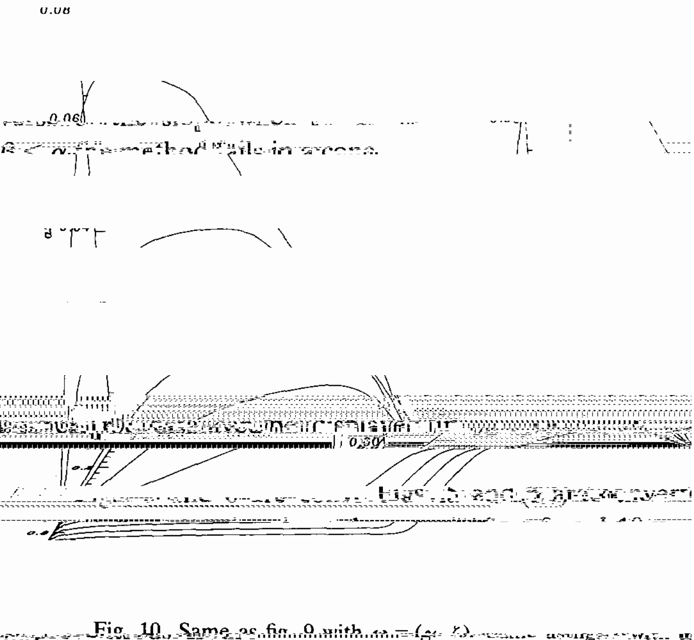

Fig. 10. Same as fig. 9 with $\omega = (\gamma, \ldots)$ ...

to determine the "last invariant torus". One

beginning at the origin. One could linearly order

definition of order.

Curve based order. An $\boldsymbol{\omega}$ torus persists longer than a $\boldsymbol{\mu}$ torus along a curve $\boldsymbol{\xi}(t)$ for which $\boldsymbol{\xi}(0) = 0$, if $\boldsymbol{\xi}(t)$ intersects the boundary of the domain of convergence of the $\boldsymbol{\mu}$ torus first.

The simplest example of a parameterized family

surface, which is all a curve based order allows. In some sense, one may want to incorporate the

torus persists longer than a $\boldsymbol{\mu}$ torus if the in-

If one surface is completely contained inside

the *partial ordering*

quencies will intersect in general, and then the

amples, the surface for (τ, τ^2) is completely con-

containment of the (γ, ζ) surface is partly due to

to compare the (γ, σ) and (γ, ζ) tori, note that though $a^{ss}(\sigma) > a^{ss}(\zeta)$, $a^{ss}(\gamma + \sigma) < a^{ss}(\gamma + \zeta)$. Thus the surfaces must intersect, and therefore there can only be parametrized comparisons.

Conclusions

We have determined the domain of existence

series in the angle variables. The semi-Froeshlé mapping has the advantage that two of the pa-

boundary of the domain for several frequency

be smooth, rather surprisingly. It appears smooth

when projected on the parameter

the uncoupled mappings. Furthermore, numerical results imply that the domain is bounded by

eq. (2). They also apply to the $2d$-dimensional

[11] J. Guckenheimer, B. Hu and J. Rudnick, Quasiperiodic Transition to Chaos with Three Incommensurate Fre-

mations in the study of dynamical systems, Phys. Rev. A

circles in area-preserving maps, Physica D 7 (1983) 283–300.

[16] R.S. McKay, On Greene's Residue Criterion, Universi-

(1992) 149–160.

Tori of Cubic Irrational Winding Number, University of Houston (1989).

[25] M. Muldoon, Ghosts of Order on the Frontier of Chaos.

ones, Russ. Math. Surveys 32:6 (1977) 1–65;
G. Benettin, L. Galgani and A. Giorgilli, A proof of Nekhoroshev's theorem for the stability times in nearly

Physica D 6 (1982) 67–77.